Far-Ultraviolet Observations of Outflows from Infrared-Luminous Galaxies

Claus Leitherer[1], Rupali Chandar[2], Christy A. Tremonti[3], and Aida Wofford[1]

[1] Space Telescope Science Institute, 3700 San Martin Dr., Baltimore, MD 21218, USA
email: `leitherer@stsci.edu`, `wofford@stsci.edu`

[2] The University of Toledo, Dept. of Physics and Astronomy, Toledo, OH 43606, USA
email: `rupali.chandar@utoledo.edu`

[3] University of Wisconsin, Dept. of Astronomy, 475 N. Charter St., Madison, WI 53706, USA
email: `tremonti@astro.wisc.edu`

Abstract. We have obtained ultraviolet spectra between 1150 and 1450 Å of four ultraviolet-bright, infrared-luminous starburst galaxies. Our selected sight-lines towards the starburst nuclei probe the conditions in the starburst-driven outflows. We detect outflowing gas with velocities of up to $\sim$900 km s^{-1}. It is likely that the outflows are a major source of metal enrichment of the galaxies' halos. The mass outflow rates of several tens of M$_\odot$ yr^{-1} are similar to the star-formation rates. The outflows may quench star formation and ultimately regulate the starburst.

Keywords. galaxies: halos — intergalactic medium — galaxies: starburst — ultraviolet: ISM

1. Introduction

The absorption spectra of quasi-stellar objects demonstrate that metals in the universe are found far from their production sites. Mg II absorbers are associated with galaxies at impact parameters well outside their luminous dimensions. Advances in ground- and space-based telescopes and detectors have pushed the discovery space to many other ions, as well as to low and high redshift (e.g., Ménard *et al.* 2011; Tumlinson *et al.* 2011a).

An alternative technique of probing the circumgalactic gas is to directly target galaxies and measure the self-absorption in their spectra. Absorption-line studies of circumgalactic gas have been performed at low (e.g., Rupke, Veilleux, & Sanders 2005a,b,c; Chen *et al.* 2010), intermediate (e.g., Weiner *et al.* 2009; Coil *et al.* 2011; Erb *et al.* 2012), and high (e.g., Pettini *et al.* 2002; Steidel *et al.* 2010) redshift.

Starburst galaxies are of particular interest. Galactic-scale outflows of gas are ubiquitous in the most actively star-forming galaxies in the local (Chen *et al.* 2010) and distant universe (Shapley *et al.* 2003). These outflows affect the evolution of galaxies and the intergalactic medium (Veilleux, Cecil, & Bland-Hawthorn 2005). For example, by selectively blowing metals out of shallow galactic potential wells, they may explain the tight relation between stellar mass and metallicity (Tremonti *et al.* 2004).

The ultraviolet (UV) is key for understanding starbursts. Previous space-UV spectroscopy has focused almost exclusively on blue, and therefore metal-poor, low-luminosity starburst galaxies but has neglected the powerful, infrared-(IR) bright (but UV-faint) nuclear starbursts. Yet, IR-bright starbursts may have very different properties in terms of their initial mass function (IMF), specific star-formation intensity, and their relation to the circumgalactic gas. We have obtained UV spectroscopy of four IR-luminous starburst galaxies whose UV brightness makes them the targets of choice for this purpose.

Table 1. Galaxy properties.

Galaxy	v_{helio} [km s^{-1}]	$\log(L_{\text{IR}})$ [L$_\odot$]	12+log(O/H)	$E(B-V)$ [mag]	SFR$_{\text{UV}}$ [M$_\odot$ yr^{-1}]
F08339+6517	5730	11.1	8.45	0.34	70
NGC 3256	2804	11.6	8.73	0.54	55
NGC 6090	8785	11.6	8.77	0.28	29
NGC 7552	1608	11.1	8.74	0.54	57

2. Sample

Naively, one would expect dusty, IR-luminous galaxies to be dauntingly faint in the UV. However, much of the dust responsible for the UV extinction is apparently distributed around the starburst in the form of a moderately inhomogeneous foreground screen (Calzetti 2001). Therefore we are able to directly study much of the stellar population responsible for powering the starburst via observations in the UV.

The selected galaxies are F08339+6517, NGC 3256, NGC 6090, and NGC 7552. No strong AGN activity has been detected in any of the galaxies. A summary of some basic properties of the galaxies is in Table 1. Their heliocentric velocities (v_{helio}) are large enough to preclude blending gas absorption lines from the target galaxy and the Milky Way.

We used the G130M mode of HST's COS. The four galaxies are nuclear starbursts, and the 2.5″ circular COS aperture (projected size ∼300 and 1600 pc) was placed on the galaxy centers. We corrected the spectra for foreground reddening and converted to restframe wavelengths. We measured the widths of the Milky Way foreground lines, which are unresolved at the nominal COS G130M resolution of R = 17,000. Typical widths are ∼0.5 Å. In Figure 1 we show the rectified spectrum of F08339+6517 as an example. We identified the major spectral features using the line list of Leitherer *et al.* (2011).

3. Internal Reddening and Stellar Populations

We applied the standard technique of UV spectral synthesis (e.g., Wofford, Leitherer, & Chandar 2011) to constrain the most recent star-formation history traced by massive OB
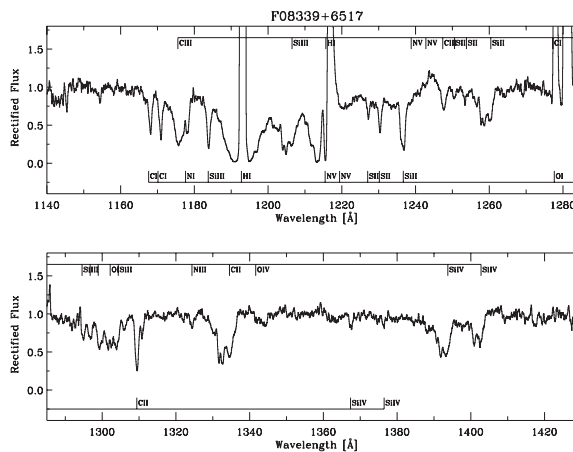

Figure 1. Rectified COS spectrum of F08339+6517. The wavelength scale is in the galaxy restframe. Milky Way lines are identified below the spectrum; galaxy lines are above.

stars. The intrinsic reddening was determined by comparing the observed UV continuum slope to the one predicted by the models. In column 5 of Table 1 we report the derived total reddening $E(B-V)$, which is the sum of the foreground and intrinsic reddening.

After dereddening the spectra with a Calzetti (2001) attenuation curve, the monochromatic UV luminosities were obtained. By extrapolating to lower masses using the adopted IMF and correcting for aperture-size effects, we derived the total star-formation rates (SFR) listed in column 6. SFR ranges between 30 and 70 $M_\odot$ yr^{-1}, which are typical values for IR-luminous galaxies. All four galaxies follow the empirical relation between the far-IR luminosity and the UV reddening (Meurer, Heckman, & Calzetti 1999).

4. Outflow Properties

Lyman-α is the strongest emission line in all four galaxies. The equivalent widths range from 2 to 13 Å, which can be compared to the value of $\sim$100 Å expected for a 20 Myr old continuous starburst under Case B conditions. This suggests a Lyman-α escape fraction of $\sim$10%. The escape probability of Lyman-α photons strongly depends on the velocity structure of the ISM and the dust content (Kunth *et al.* 1998; Charlot & Fall 1993). Although our sample is small, we note the absence of any correlation with reddening.

Schaerer *et al.* (2011) generated a library of theoretical Lyman-α profiles formed in the moving media of star-forming galaxies. These profiles are useful for determining the column densities, kinematics, and dust content of the neutral ISM along the sight-lines to the nuclear starbursts. Comparison with the observed profiles suggests H I column densities of order 10^{20} cm^{-2}.

The strongest absorption features are the low-ionization lines of Si III $\lambda1206$, Si II $\lambda1260$, and C II $\lambda1334$. Inspection of the line profiles suggests a complex structure with several components present. We used the Galactic foreground lines as fiducials to verify that the observed profiles are not affected by artifacts. The profiles are blueshifted and composed of several discrete components with velocities of up to $\sim$900 km s^{-1}. The bulk

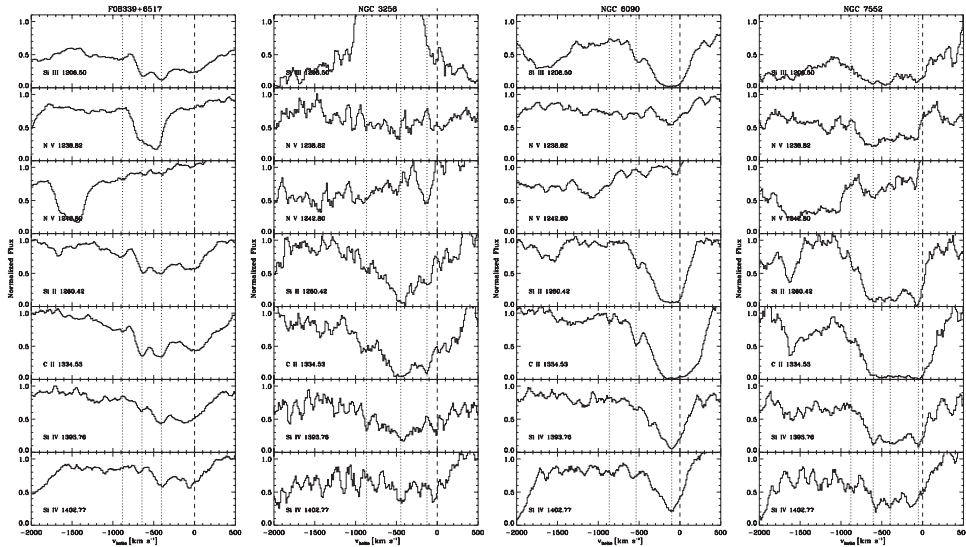**Figure 2.** Continuum-normalized absorption profiles versus $v_{\rm helio}$ for F08339+6517, NGC 3256, NGC 6090, and NGC 7552 (from left to right). The lines are from top to bottom: Si III $\lambda1206$, Si II $\lambda1260$, C II $\lambda1334$, Si IV $\lambda1393$, and Si IV $\lambda1402$. The dashed vertical line indicates zero velocity. Dotted vertical lines indicate discrete components at velocities up to $\sim$900 km s^{-1}.

velocities are around 500 km s^{-1}. This is illustrated in Figure 2, where we plot Si III, Si II, C II and other lines (discussed below) in velocity space with the detected components highlighted. We chose a conservative approach and dismissed structures whose origin could not clearly be attributed to a high-velocity component in all three lines. For instance a strong absorption at 1324 Å is more likely due to N III λ1324.35 rather than blueshifted C II. Given the redshift of the four galaxies, we can confidently rule out any confusion with Galactic high-velocity clouds. Higher-ionization lines, such as Si IV λ1400 and N V λ1240 show P Cygni profiles due to stellar winds. The wind signatures preclude firm conclusions on the presence of the features detected in the low-ionization lines.

The most natural interpretation of the observed velocity structure is expanding warm ($\sim$10^4 K) gas driven by the current burst of star formation. The individual components indicate density inhomogeneities of the outflow, as expected for interstellar material entrained in a galactic-scale wind. The flow time scale of $\sim$10 Myr (for an assumed size of 5 kpc and $v = 500$ km s^{-1}) corresponds to the typical duration of starbursts. Does the material escape from the gravitational well of the galaxies? The observed maximum outflow velocities of the four galaxies are similar to the escape velocities for an assumed halo extending to 100 kpc . Therefore it is not likely that the material will escape from the galaxy potential. Instead it may accumulate in the halo, which serves as a reservoir for newly formed metals (Tumlinson *et al.* 2011b).

Following Heckman *et al.* (2000), Rupke *et al.* (2005a,b,c), and Weiner *et al.* (2009), we can estimate the mass outflow rates from the observed H I columns, the characteristic length scale, and the outflow velocities: $\dot{M} = 22$ M$_\odot$ yr^{-1} $\frac{N_\mathrm{H}}{10^{20}\mathrm{cm}^{-2}}$ $\frac{R}{5\mathrm{kpc}}$ $\frac{v}{300\mathrm{km\ s}^{-1}}$. The rates of $10^1 - 10^2$ M$_\odot$ yr^{-1} are similar to the star-formation rates. Therefore, the outflows may quench star formation and ultimately regulate the starburst.

References

Calzetti, D. 2001, *PASP*, 113, 1449

Charlot, S. & Fall, S. M. 1993, *ApJ*, 415, 580

Chen, Y.-M., Tremonti, C. A., Heckman, T. M., *et al.* 2010, *AJ*, 140, 445

Coil, A. L., Weiner, B. J., Holz, D. E., *et al.* 2011, *ApJ*, 743, 46

Heckman, T. M., Lehnert, M. D., Strickland, D. K., & Armus, L. 2000, *ApJS*, 129, 493

Erb, D. K., Quider, A. M., Henry, A. L., & Martin, C. L. 2012, arXiv:1209.4903

Kunth, D., Mas-Hesse, J. M., Terlevich, E., *et al.* 1998, *A&A*, 334, 11

Leitherer, C., Tremonti, C. A., Heckman, T. M., & Calzetti, D. 2011, *AJ*, 141, 37

Ménard, B., Wild, V., Nestor, D., *et al.* 2011, *MNRAS*, 417, 801

Meurer, G. R., Heckman, T. M., & Calzetti, D. 1999, *ApJ*, 521, 64

Pettini, M., Rix, S. A., Steidel, C. C., Adelberger, K. L., Hunt, M. P., & Shapley, A. E. 2002, *ApJ*, 569, 742

Rupke, D. S., Veilleux, S., & Sanders, D. B. 2005a, *ApJS*, 160, 87

——. 2005b, *ApJS*, 160, 115

——. 2005c, *ApJ*, 632, 751

Schaerer, D., Hayes, M., Verhamme, A., & Teyssier, R. 2011, *A&A*, 531, A12

Shapley, A. E., Steidel, C. C., Pettini, M., & Adelberger, K. L. 2003, *ApJ*, 588, 65

Steidel, C. C., Erb, D. K., Shapley, A. E., *et al.* 2010, *ApJ*, 717, 289

Tremonti, C. A., Heckman, T. M., Kauffmann, G., *et al.* 2004, *ApJ*, 613, 898

Tumlinson, J., Thom, C., Werk, J. K., *et al.* 2011b, *Science*, 334, 948

Tumlinson, J., Werk, J. K., Thom, C., *et al.* 2011a, *ApJ*, 733, 111

Veilleux, S., Cecil, G., & Bland-Hawthorn, J. 2005, *ARA&A*, 43, 769

Weiner, B. J., Coil, A. L., Prochaska, J. X., *et al.* 2009, *ApJ*, 692, 187

Wofford, A., Leitherer, C., & Chandar, R. 2011, *ApJ*, 727, 100